Influences of different oxidants on characteristics of La_2O_3/Al_2O_3 nanolaminates deposited by atomic layer deposition*

Ji-Bin Fan(樊继斌)[1,†], Hong-Xia Liu(刘红侠)[2], Li Duan(段理)[1], Yan Zhang(张研)[1], and Xiao-Chen Yu(于晓晨)[1]

[1] School of Materials Science and Engineering, Chang'an University, Xi'an 710061, China
[2] School of Microelectronics, Key Laboratory of Wide Band-Gap Semiconductor Materials and Devices, Xidian University, Xi'an 710071, China

(Received 30 November 2016; revised manuscript received 27 February 2017; published online 20 April 2017)

A comparative study of two kinds of oxidants (H_2O and O_3) with the combination of two metal precursors (TMA and La(^{i}PrCp)$_3$) for atomic layer deposition (ALD) La_2O_3/Al_2O_3 nanolaminates is carried out. The effects of different oxidants on the physical properties and electrical characteristics of La_2O_3/Al_2O_3 nanolaminates are studied. Initial testing results indicate that La_2O_3/Al_2O_3 nanolaminates could avoid moisture absorption in the air after thermal annealing. However, moisture absorption occurs in H_2O-based La_2O_3/Al_2O_3 nanolaminates due to the residue hydroxyl/ hydrogen groups during annealing. As a result, roughness enhancement, band offset variation, low dielectric constant and poor electrical characteristics are measured because the properties of H_2O-based La_2O_3/Al_2O_3 nanolaminates are deteriorated. Addition thermal annealing effects on the properties of O_3-based La_2O_3/Al_2O_3 nanolaminates indicate that O_3 is a more appropriate oxidant to deposit La_2O_3/Al_2O_3 nanolaminates for electron devices application.

Keywords: La_2O_3/Al_2O_3 nanolaminates, atomic layer deposition, oxidants, annealing

PACS: 77.55.D–, 82.80.Pv **DOI:** 10.1088/1674-1056/26/6/067701

1. Introduction

Recently, rare earth oxides such as La-based binary or ternary compounds, have received a lot of attention for their potential use as second generation high dielectric constant materials instead of the currently used Hf-based dielectrics in complementary metal–oxide–semiconductor technology.[1–5] Among these rare earth oxides, lanthanum oxide is considered to be a potential candidate due to its superior properties such as a high dielectric constant (>26), large band gap (>5.8 eV) and high electrical breakdown field strength.[6,7] It is also considered to overcome the low crystallization temperature problems with other high-κ dielectrics such as HfO_2, as it has a high crystallization temperature of >900 °C.[8,9] To meet the requirements for the dielectric quality improving and thickness scaling, atomic layer deposition (ALD) has become the preferred industrial deposition technique for high-κ oxides because of its low deposition temperature, excellent thickness and composition control, and conformal growth.[10] However, due to the well-known hygroscopic nature of La_2O_3, H_2O used as an oxidant in ALD process can negatively affect the La_2O_3 growth step, and consequently also the properties of the thin film. To solve the above problems, ultraviolet ozone post treatment, capping layer, and other metal elements such as Al and Zr adopted into La_2O_3 have been studied to suppress the moisture absorption.[11–13] Besides these methods, other metal elements incorporated into La_2O_3 shows advantages in the scaling of thickness and in the controlling of properties such as dielectric constant, corrosion resistance and thermal stability. However, the oxidants' (H_2O or O_3) effects on the characteristics of metal elements incorporated with La_2O_3 have not been discussed. Different oxidants used in the ALD process have a great influence on the defects and residual impurities in the high-κ films if the process conditions are optimized.[10,14] Since this topic can be crucial for the successful inclusion of high-κ dielectrics in electron devices, the oxidant effects on the characteristics of metal element adopted La-based ternary compounds should be investigated.

In this paper, different oxidants (H_2O and O_3) are used to deposit La_2O_3/Al_2O_3 nanolaminates by the periodic stacking of bilayer structures on Si substrate by using the ALD technique at 300 °C. The effects of different oxidants on the physical properties and electrical characteristics of La_2O_3/Al_2O_3 nanolaminates are investigated after annealing.

2. Experiment

Prior to the deposition, 8–12 Ω·cm P-type Si (100) wafers were RCA cleaned and a 30-s dip in diluted HF solution was used to remove the native oxide, followed by a 60-s rinse in deionized water. Tris(isopropylcyclopentadienyl) lanthanum[La(^{i}PrCp)$_3$] was used as the lanthanum precursor

*Project supported by the National Natural Science Foundation of China (Grant Nos. 61604016 and 51501017) and the Fundamental Research Funds for the Central Universities, China (Grant No. 310831161003).

†Corresponding author. E-mail: jbfan@chd.edu.cn

© 2017 Chinese Physical Society and IOP Publishing Ltd

and trimethylaluminum (TMA) was utilized as the aluminum precursor. The container of lanthanum precursor was heated to 180 °C and aluminum precursor was at room temperature, corresponding to a vapor pressure of 10 hPa to 15 hPa. When H_2O was used as the oxidant, the container was set at room temperature, corresponding to a vapor pressure of 7 hPa. The ozone generator used the ultra pure O_2 (99.999%) to obtain O_3, the concentration was 200 g/Nm^3. La_2O_3/Al_2O_3 nanolaminates were formed by the periodic stacking of bilayer structures to form thicker multilayers. Different thickness La_2O_3/Al_2O_3 nanolaminates were deposited on Si substrates by ALD using different metal processors (La(^{i}PrCp)$_3$, TMA) and oxidants (O_3, H_2O) at 300 °C. After all the nanolaminates were annealed in the nitrogen at 600 °C for 60 s, the x-ray photoelectron spectroscopy (XPS), atomic force microscope (AFM) and electrical measurements were carried out to investigate the characteristics of the different processed La_2O_3/Al_2O_3 nanolaminates.

3. Results and discussion

Figure 1 shows the XPS spectra of the La_2O_3/Al_2O_3 nanolaminates grown using different oxidants before and after annealing. As shown in Fig. 1(a), for H_2O-based ALD process, the main peaks are La, Al, and O, the subordinate peak is C. The remaining peaks are mainly attributed to the Si substrate and Auger peaks. An obvious change is observed in the spectrum after annealing. For the O_3-based ALD process as shown in Fig. 1(b), the main peaks are La, Al, and O, and the subordinate peak is C. The remaining peaks are mainly attributed to the Si substrate and Auger peaks. After annealing, the variation in the spectrum is negligible. The results indicate that La_2O_3/Al_2O_3 nanolaminates with low impurity levels are obtained by ALD using different oxidants. A small composition variation of O_3-based La_2O_3/Al_2O_3 nanolaminate is observed compared with that of H_2O-based La_2O_3/Al_2O_3 nanolaminate after annealing.

The composition variations of XPS spectra for the La_2O_3/Al_2O_3 nanolaminates before and after annealing can be explained by the percentage composition of atomic atom variation, which is shown in Table 1. For the H_2O-based ALD process, the percentage composition of atomic atom ratio of La:Al:O is close to 1:1:3 and it changes to almost 1:2:5 after annealing. Meanwhile, the C impurity decreases from 2.3 to 1.24 after annealing. The excess oxygen after annealing may be attributed to the hygroscopicity of the La-based material leading to the incorporation of the related OH groups. For the O_3-based ALD process, the percentage compositions of atomic atoms ratio of La:Al:O are both close to 1:1:3 before and after annealing. The C impurity decreases from 1.3 to 0.69 after annealing. The results indicate that stoichiometric La_2O_3/Al_2O_3 nanolaminates are deposited for both O_3 and H_2O as oxidants if the deposition process is optimized. After annealing, the difference may be explained as follows. Owing to H_2O tending to physisorb on the surface strongly and contributing to a high concentration hydroxyl/hydrogen groups in the films although the purge time is sufficiently long,[14] the intermixing reaction occurs during the annealing, accompanied by the decomposition and re-composition of unstable bonds or groups residing in the nanolaminates. However, O_3 is easy to purge and no hydroxyl species reside in the films compared with H_2O. Therefore, the obvious change is observed in the XPS spectra.

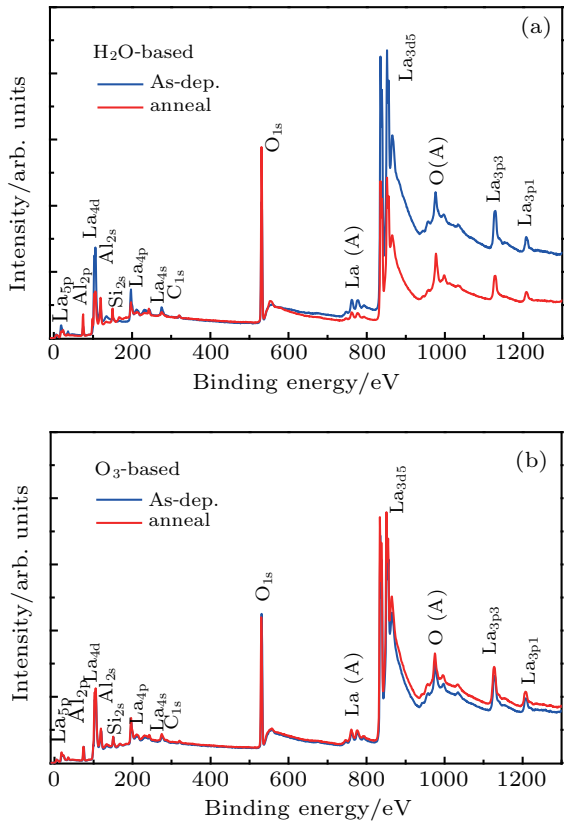


Fig. 1. (color online) XPS spectra of La_2O_3/Al_2O_3 nanolaminates grown using different oxidants before and after annealing.

Table 1. Percentage compositions of atomic atoms in La_2O_3/Al_2O_3 nanolaminates.

		La_{3d}/at.%	Al_{2p}/at.%	O_{1s}/at.%	C_{1s}/at.%	N_{1s}/at.%
H_2O-based	As-dep.	17.94	20.27	59.49	2.30	0
	anneal	12.23	22.95	63.58	1.24	0
O_3-based	As-dep.	19.23	21.86	57.61	1.30	0
	anneal	21.50	21.00	56.81	0.69	0

Figure 2 shows the O_{1s} spectra of La_2O_3/Al_2O_3 nanolaminates deposited by ALD using different oxidants. For H_2O-based ALD process, the O_{1s} core level spectrum consists of five fitting peaks, which are located at binding energies of 529.18 eV, 530.18 eV, 531.13 eV, 532.28 eV, and 533.17 eV. These peaks correspond to the chemical bonds of La–O–La, La–O–Al, Al–O–Al, La–O–H, and O–C, respectively.[11] After annealing, the peak intensity of La–O–H chemical bond increases obviously and the peak of O–C chemical bond diminishes. It can be concluded that the formation of $La(OH)_x$ occurs during annealing due to the residue of hydroxyl/hydrogen groups in the layers. For O_3-based ALD process, the O_{1s} core level spectrum consists of three fitting peaks, which are located at the binding energies of 528.94 eV, 530.40 eV, and 531.68 eV, respectively. These peaks are corresponding to the chemical bonds of La–O–La, La–O–Al, and Al–O–Al, respectively.[11] After annealing, no obvious change is observed except the variation of peak intensity due to the diffusion of atoms.

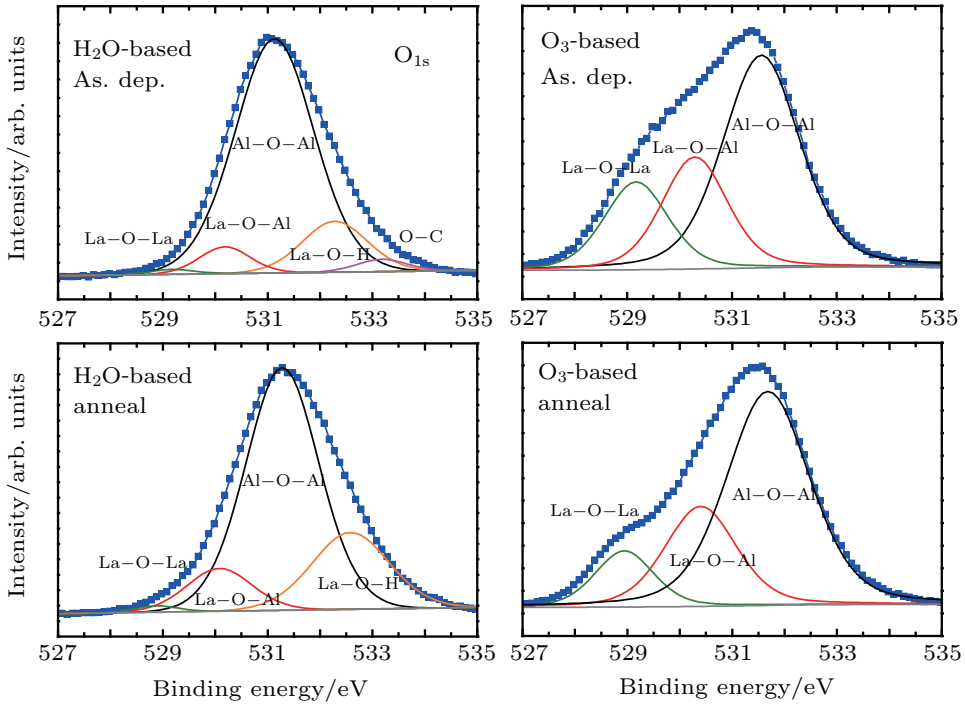


Fig. 2. (color online) O_{1s} spectra of La_2O_3/Al_2O_3 nanolaminates deposited by ALD using different oxidants.

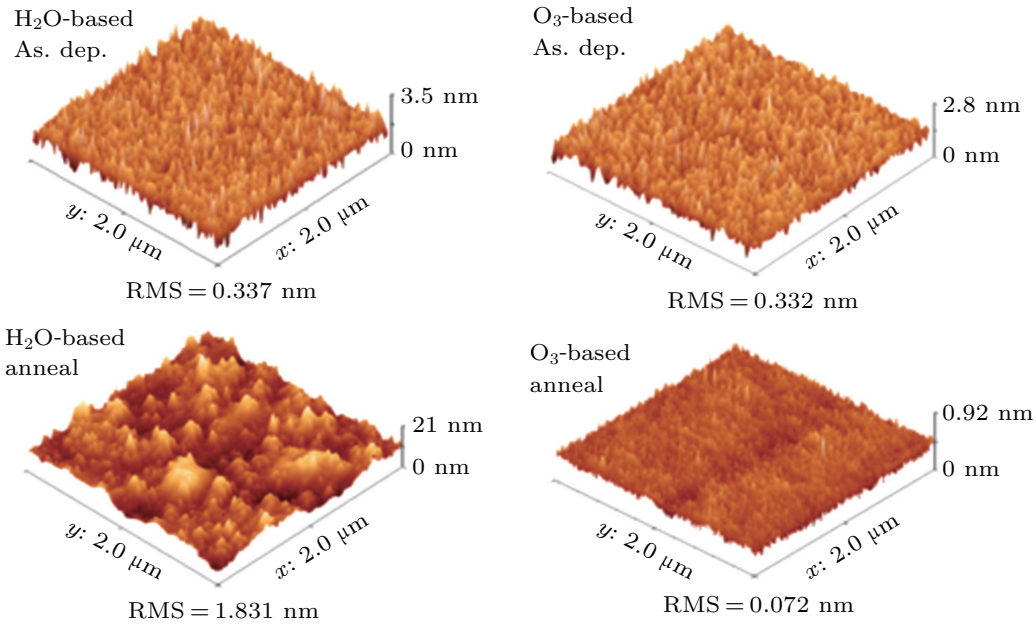


Fig. 3. (color online) AFM surface images of La_2O_3/Al_2O_3 nanolaminates deposited by ALD using different oxidants.

Figure 3 shows the surface roughnesses of the La_2O_3/Al_2O_3 nanolaminates before and after annealing. As shown in Fig. 3, the root mean square (RMS) roughness of the H_2O-based nanolaminate increases sharply from 0.337 nm to 1.831 nm after annealing, whereas that of the O_3-based nanolaminate decreases from 0.332 nm to 0.072 nm. The RMS value of H_2O-based nanolaminate increases nearly 5.4 times after annealing possibly due to the formation of low density hexagonal $La(OH)_3$.[15] Meanwhile, due to the densification of the nanolaminate after annealing, the RMS value of O_3-based nanolaminate decreases nearly twice. The results suggest that the La_2O_3/Al_2O_3 nanolaminates deposited by ALD using H_2O as oxidant still suffer from moisture absorption of La_2O_3 due to the residual hydroxyl/hydrogen groups, which is harmful to obtaining the good properties of La_2O_3/Al_2O_3 nanolaminates after annealing.

In order to evaluate the oxidant effects on the properties of La_2O_3/Al_2O_3 nanolaminates before and after annealing, the valence band offset (VBO) is determined by using the method proposed by Kraut[16]

$$\Delta E_{\mathrm{VBO}} = \left(E_{\mathrm{CL}}^{\mathrm{Si_{2p}}} - E_{\mathrm{V}}\right)_{\mathrm{bulk,Si}} - \left(E_{\mathrm{CL}}^{\mathrm{Al_{2p}}} - E_{\mathrm{V}}\right)_{\mathrm{thick\ nanolaminate}} - \left(E_{\mathrm{CL}}^{\mathrm{Si_{2p}}} - E_{\mathrm{CL}}^{\mathrm{Al_{2p}}}\right)_{\mathrm{thin\ nanolaminate/Si}}, \quad (1)$$

where $E_{\mathrm{CL}}^{\mathrm{Si_{2p}}}$ and $E_{\mathrm{CL}}^{\mathrm{Al_{2p}}}$ are the binding energies of the Si_{2p} and Al_{2p} shallow core levels, respectively, and E_{V} is the binding energy corresponding to the valence band maximum (VBM). The position of the VBM is determined by using the linear method. The energy differences between these core levels and the corresponding valence band maxima E_{V} in bulk Si and thick La_2O_3/Al_2O_3 nanolaminate are determined. By measuring the energy difference between two shallow core levels in thin nanolaminates on Si, the VBO of the La_2O_3/Al_2O_3 nanolaminates can be calculated. Figure 4 shows the core-level spectrum of Si_{2p} for bulk clean Si sample measured by XPS. The energy difference between the Si_{2p} and VBM is 98.90 eV, which accords well with that in the early work.[10]

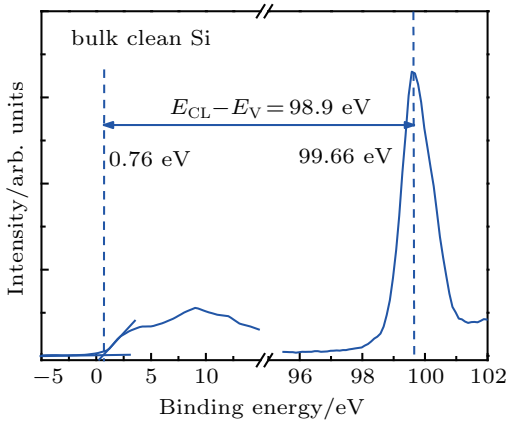


Fig. 4. (color online) The XPS core-level spectrum of Si_{2p} for bulk clean Si.

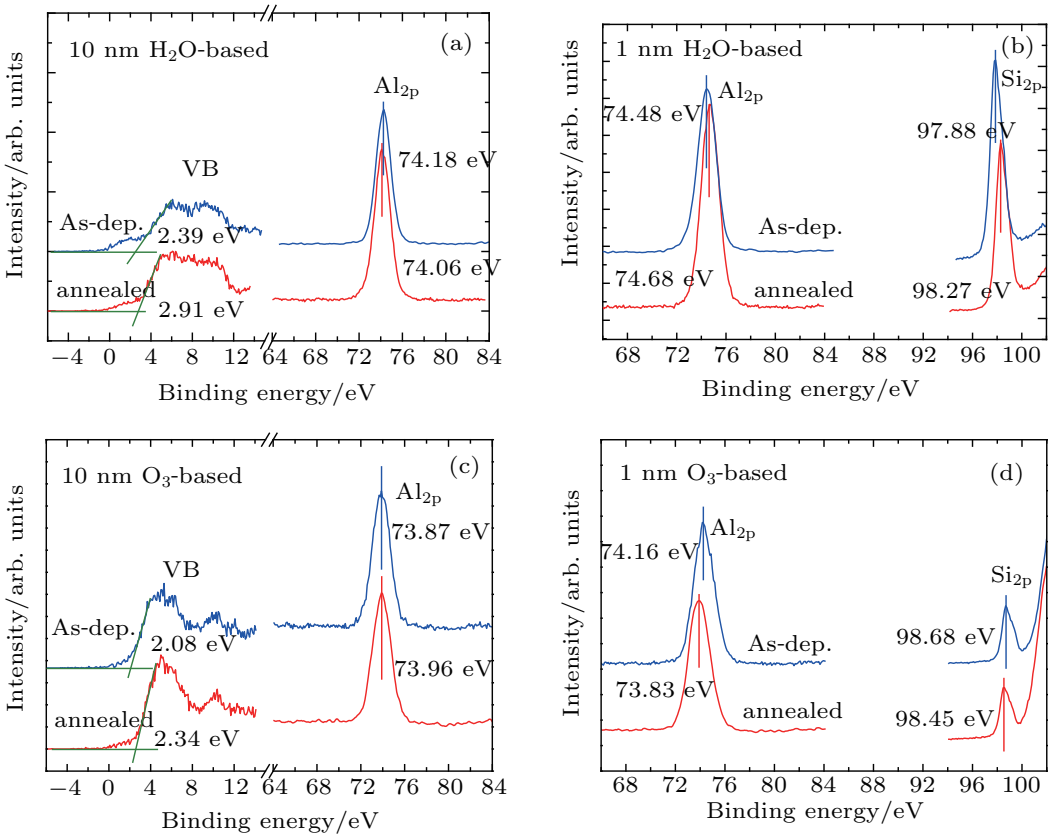


Fig. 5. (color online) The XPS core-level spectra of Si_{2p} and Al_{2p} for 10-nm and 1-nm La_2O_3/Al_2O_3 nanolaminates before annealing (As-dep.) and after annealing (being annealed).

Figure 5 shows the XPS core-level spectra of Si_{2p} and Al_{2p} for La_2O_3/Al_2O_3 nanolaminates deposited by ALD using different oxidants. The core level energies are obtained by curve fitting to ensure high accuracy binding energy of the peak, and the spectra are referenced to the C_{1s} peak at 284.8 eV. For the H_2O-based ALD process, the energy difference between the Al_{2p} and VBM decreases from 71.79 eV to 71.15 eV after annealing as shown in Fig. 5(a). The energy differences between Al_{2p} and Si_{2p} are 23.40 eV and 23.59 eV for the as-deposited and the annealed thin nanolaminates, respectively, as shown in Fig. 5(b). Using these values with Eq. (1), we obtain a VBO of 3.71 eV and 4.16 eV for the as-deposited and the annealed La_2O_3/Al_2O_3 nanolaminates, respectively. The VBO value increases 0.45 eV after annealing which may be related to the vacancies generated due to the moisture absorption of La_2O_3. For the O_3-based ALD process, the energy difference between the Al_{2p} and VBM decreases from 71.79 eV to 71.62 eV after annealing, as shown in Fig. 5(c). The energy difference between Al_{2p} and Si_{2p} was 24.52 eV and 24.62 eV for the as-deposited and the annealed thin nanolaminates, respectively, as shown in Fig. 5(d). Substituting these values into Eq. (1), the values of VBO of 2.59 eV and 2.66 eV are obtained for the as-deposited and the annealed La_2O_3/Al_2O_3 nanolaminates, respectively. The negligible variation of VBO value for O_3-based La_2O_3/Al_2O_3 nanolaminates is observed after annealing.

The band offset change after annealing should result in a shift in V_{FB}.[17,18] Figure 6 shows the *C*–*V* characteristics of 5-nm La_2O_3/Al_2O_3 nanolaminates deposited by ALD with using different oxidants before and after annealing (f = 100 kHz). The gate voltage (V_G) is swept from accumulation to inversion and then swept back. For the H_2O-based ALD process as shown in Fig. 6(a), the hysteresis in the *C*–*V* curve increases significantly and the capacitance value of La_2O_3/Al_2O_3 nanolaminates decreases after annealing. It can be explained by the fact that the moisture absorption of La_2O_3 deteriorates the properties of nanolaminates, such as the increase of nanolaminate roughness, degradation of density and formation of $La(OH)_3$ with a low permittivity.[15] Furthermore, the *C*–*V* curve shifts from the positive to the negative direction after annealing, showing that the positive charge increases after annealing, which is associated with the generation of oxygen vacancies.[19,20] The permittivity obtained for H_2O-based La_2O_3/Al_2O_3 nanolaminate is 9.6 and it decreases to 6.7 after annealing. For the O_3-based ALD process, due to the densification of La_2O_3/Al_2O_3 nanolaminates and decrease of the impurity concentration, the *C*–*V* characteristics of La_2O_3/Al_2O_3 nanolaminates improve after annealing as shown in Fig. 6(b). Furthermore, the capacitance value decreases after annealing, which may be attributed to the low dielectric interfacial layer thickness between La_2O_3/Al_2O_3 nanolaminates and Si substrate increasing. Moreover, a hump appears in the *C*–*V* curve and it disappears after thermal annealing process. It can be explained by the fact that the traps or defects are generated in the nanolaminate due to the strong oxidization and lability of O_3.[21] Thermal annealing supplies enough thermal energy for the decomposition and re-composition of traps or defects, the traps or defects decrease and the hump disappears after annealing. The permittivities obtained for the as-deposited and annealed O_3-based La_2O_3/Al_2O_3 nanolaminate are 14.4 and 13.7, respectively.

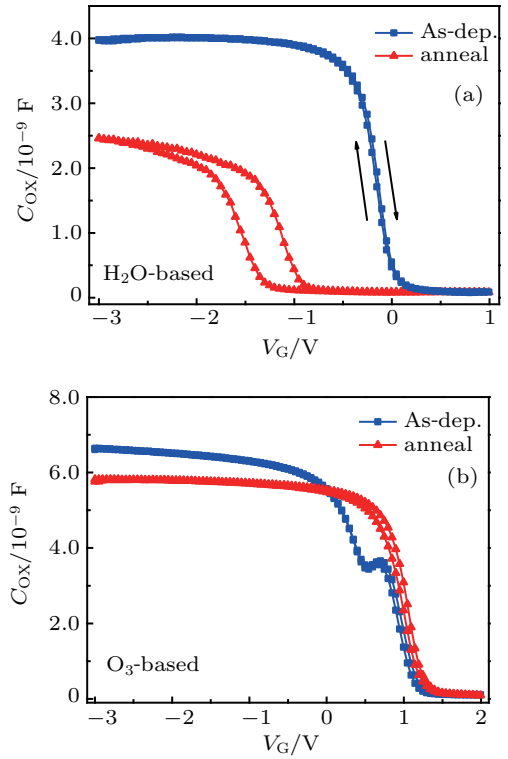


Fig. 6. (color online) The *C*–*V* characteristics of La_2O_3/Al_2O_3 nanolaminates deposited by ALD with different oxidants before and after annealing (f = 100 kHz).

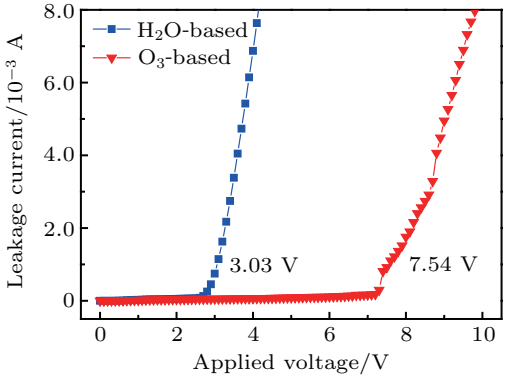


Fig. 7. (color online) Breakdown characteristics of Al/La_2O_3/Al_2O_3 nanolaminates/Si MIS capacitors with different oxidants.

Breakdown characteristics of the Al/5 nm La_2O_3/Al_2O_3 nanolaminate/p-type Si/Al capacitor structure are shown in Fig. 7. The capacitor with H_2O-based La_2O_3/Al_2O_3 nanolaminate shows considerably low breakdown voltage due to the

moisture absorption deteriorating the properties of nanolaminates. A high breakdown voltage of 7.54 V for the capacitor with O_3-based La_2O_3/Al_2O_3 nanolaminate is measured at a leakage current of 1 mA while that of the H_2O-based La_2O_3/Al_2O_3 nanolaminate is 3.03 V. The breakdown voltage improvement results from the suppressed moisture absorption, which is consistent with the *C*–*V* measurement results.

4. Conclusions

Preliminary results in the development of ALD-grown La_2O_3/Al_2O_3 nanolaminates for serving as dielectric are presented. The oxidants' (H_2O and O_3) effects on the physical properties and electrical characteristics of La_2O_3/Al_2O_3 nanolaminates are investigated. The XPS results indicate that compared with the O_3-based process, La_2O_3/Al_2O_3 nanolaminates grown with H_2O used as an oxidant suffer the moisture absorption of La_2O_3 after thermal annealing due to the relatively high residue level of hydroxyl/hydrogen groups. As a result, a large valence band offset is observed and the surface roughnesses of La_2O_3/Al_2O_3 nanolaminates increase significantly due to the formation of low density hexagonal $La(OH)_3$. Further electrical measurement shows that the electrical characteristics of H_2O-based La_2O_3/Al_2O_3 nanolaminates are deteriorated and low permittivity and breakdown voltage are achieved. All results indicate that O_3 is a more appropriate oxidant to deposit La_2O_3/Al_2O_3 nanolaminates for electronic device applications.

References

[1] Gupta S, Gong X, Zhang R, Yeo Y C, Takagi S and Saraswat K C 2014 *MRS Bull.* **39** 678

[2] McDaniel M D, Ngo T Q, Hu S, Posadas A, Demkov A A and Ekerdt J G 2015 *Appl. Phys. Rev.* **2** 041301

[3] Bere M K, Liu Y, Kyaw L M, Ngoo Y J, Singh S P and Chor E F 2014 *ECS Trans.* **61** 271

[4] Ma L T, Fan H Q, Wang J, Zhao Y W, Tian H L and Dong G Z 2016 *Appl. Catal. B Environ.* **190** 93

[5] Ma L T, Fan H Q, Li M M, Tian H L, Fang J W and Dong G Z 2015 *J. Mater. Chem. A* **3** 22404

[6] Choi M, Janotti A and Walle C G V D 2013 *Phys. Rev. B* **88** 330

[7] Klenov D O, Schlom D G, Li H and Stemmer S 2005 *Jpn. J. Appl. Phys.* **44** 617

[8] Yang C, Fan H Q, Qiu S J, Xi Y X and Fu Y F 2009 *J. Non-Cryst. Solids* **355** 33

[9] Yang C, Fan H Q, Qiu S J, Xi Y X and Fu Y F 2008 *Surf. Rev. Lett.* **15** 271

[10] Fan J B, Liu H X, Ma F, Zhuo Q Q and Hao Y 2013 *Chin. Phys. B* **22** 027702

[11] Zhao Y, Kita K, Kyuno K and Toriumi A 2007 *Jpn. J. Appl. Phys.* **46** 4189

[12] Kukli K, Ritala M, Pore V, Leskel M, Sajavaara T, Hegde R I, Gilmer D C, Tobin P J, Jones A C and Aspinall H C 2006 *Chem. Vap. Deposition* **12** 158

[13] Li H, Shenai D V, Pugh R and Kim J 2007 *Mater. Res. Soc. Symp. Proc.* **41** 1036

[14] Fan J B, Liu H X, Gao B, Ma F, Zhuo Q Q and Hao Y 2012 *Chin. Phys. B* **21** 087702

[15] Zhao Y, Toyama M, Kita K, Kyuno K and Toriumi A 2006 *Appl. Phys. Lett.* **88** 072904

[16] Kraut E A, Grant R W, Waldrop J R and Kowalczyk S P 1983 *Phys. Rev. B* **28** 1965

[17] Fortunato E, Barquinha P and Martins R. 2012 *Adv. Mater.* **24** 2945

[18] Chang I Y, You S, Juan P, Wang M and Lee J Y 2009 *IEEE Electron Dev. Lett.* **30** 161

[19] Armacost M, Augustin A, Felsner P, Feng Y, Friese G, Heidenreich J, Hueckel G, Prigge O and Stein K 2000 *Tech. Dig.- Int. Electron Devices Meeting*, pp. 157–160

[20] Woo J C, Chun Y S, Joo Y H and Kim C I 2012 *Appl. Phys. Lett.* **100** 081101

[21] Fan J B, Liu H X, Kuang Q W, Gao B, Ma F and Hao Y 2012 *Microelectron. Reliab.* **52** 1043